Engineering Failure Analysis 18 (2011) 271–283

Contents lists available at ScienceDirect

Engineering Failure Analysis

journal homepage: www.elsevier.com/locate/engfailanal

Corrosion defect assessment on pipes using limit analysis and notch fracture mechanics ☆

M. Hadj Meliani [a,c,*], Y.G. Matvienko [b], G. Pluvinage [c]

[a] Laboratoire de Physique Théorique et Physique des Matériaux (LPTPM), FSSI, Université Hassiba Benbouali-Chlef-02000, Algeria
[b] Laboratory of Modelling Damage and Fracture, Mechanical Engineering Research Institute of the Russian Academy of Sciences, 4 M. Kharitonievsky Per., 101990 Moscow, Russia
[c] Laboratoire de Mécanique, Biomécanique, Polymères et structures, LaBPS-ENIM, île de Saulcy 57045, Université Paul Verlaine de Metz, France

ARTICLE INFO

Article history:
Received 16 May 2010
Received in revised form 13 September 2010
Accepted 13 September 2010
Available online 22 September 2010

Keywords:
Limit analysis
Notch modified failure assessment diagram
Safety factor
Probability of failure

ABSTRACT

Two methods of corrosion defect assessment on pipes are described: limit analysis (LA) and notch modified failure assessment diagram (NMFAD). Limit pressure analysis are based on ASME B31G, modified ASME B31G, DNV RP-F101 codes and recent proposed formulation. The notch stress intensity factor concept and SINTAP structural integrity procedure are combined to assess pipelines integrity into a notch-based assessment diagram so-called 'NFAD'. Defect assessment is made by comparing safety factor to a prescribed value (deterministic approach) or probability of failure to a conventional level.

1. Introduction

Pipelines have been employed as one of the most practical and low price method for large oil and gas transport since 1950. The pipe line installations for oil and gas transmission are drastically increased in last three decades. Consequently, the pipeline failure problems have been increasingly occurred. The economical and environmental and eventually in human life considerations involve the current issue as structural integrity and safety affair. The explosive characteristics of gas provide high wakefulness about the structural integrity. Therefore, the reliable structural integrity and safety of oil and gas pipelines under various service conditions including presence of defects should be warily evaluated. The external defects, e.g., corrosion defects, gouge, foreign object scratches, and pipeline erection activities are major failure reasons of gas pipelines. A typical example of a corrosion defect is given in Picture 1. According to numerous design codes, this kind of defects is considered as a semi-elliptical crack-like surface defect of aspect ratio a/c. The aspect ratio varies in range [0.1–1] depending on corrosion rate anisotropy. Several types of pipes failures can be distinguished as longitudinal, circumferential or helicoidally failures. These types depend mainly on pipe diameter. For small diameter pipes, where bending stresses are predominant, circumferential failure occurs. For large diameters, hoop stresses are more important than bending stresses and longitudinal failure appears. When bending and hoop stresses are of the same importance, fracture path becomes spiraled.

Pipe steels have yield stress up to 700 MPa for the most recent quality in order to ensure enough ductility and weldability. Failures emanating from corrosion defect are elasto plastic fracture or plastic collapse. For these two situations, defect assessment is made generally by two tools: failure assessment diagram (FAD) and limit analysis (LA).

☆ The Paper was presented by Prof. G. Pluvinage at the Nato-Workshop Biskra, Algeria, 26–28 April 2010.

* Corresponding author.
E-mail address: hadjmeliani@univ-metz.fr (M. Hadj Meliani).

1350-6307/$ - see front matter © 2010 Elsevier Ltd. All rights reserved.
doi:10.1016/j.engfailanal.2010.09.006

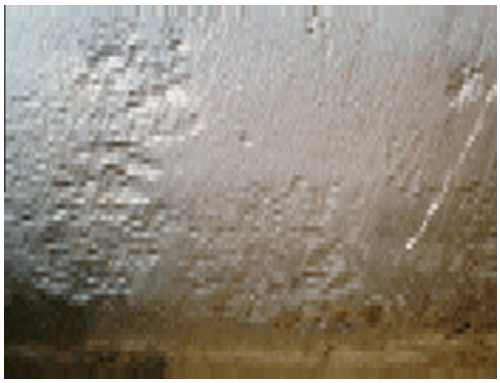

Picture 1. Example of corrosion defect on pipe.

In this paper the two major corrosion defect assessment tools for pipes are presented:

(i) limit analysis
(ii) a notch adapted failure assessment diagram by modification of the SINTAP procedure using the volumetric method, a comparison of the methods is given as a conclusion.

2. Assessment of corrosion defect by limit analysis

The structural integrity of corrosion defects is substantially studied. In Fig. 1, a list of methods available for corrosion defect assessment is presented. They are grouped vertically by their type, codified methods or others, and horizontally by their applicability, pressure or combined loading, etc.

2.1. ASME B31G and modified ASME B31G

ASME B31G [1] is a code for evaluating the remaining strength of corroded pipelines. It is a supplement to the ASME B31 code for pressure piping. The code was developed in the late 1960s and early 1970s at Battelle Memorial Institute and provides a semi-empirical procedure for the assessment of corroded pipes. Based on an extensive series of full-scale

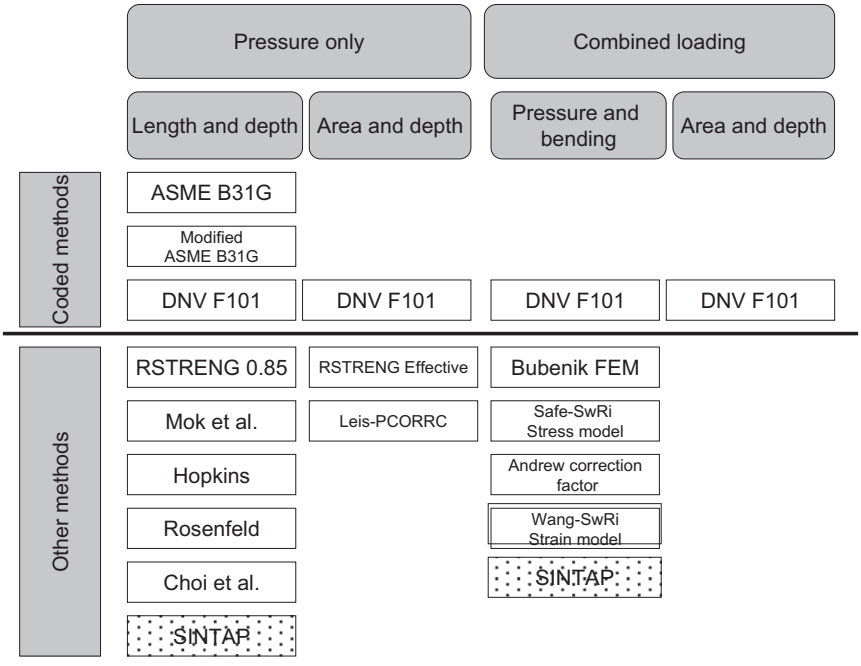

Fig. 1. Methods for corrosion defect assessment based on limit analysis.

tests on corroded pipe sections, it was concluded that pipeline steels have adequate toughness and the toughness is not a significant factor. The failure of blunt corrosion flaws is controlled by their size and the flow stress or yield stress of the material. The input parameters include pipe outer diameter (D) and wall thickness (t), the specified minimum yield strength (σ_Y), the maximum allowable operating pressure (MAOP), longitudinal extent of corrosion (L_c) and defect depth (d).

According to the ASME B31G code, a failure equation for corroded pipelines was proposed by means of data of burst experiments and expressed with consideration of two conditions below. First, the maximum hoop stress cannot exceed the yield strength of the material ($\sigma_{\theta\theta} \leqslant \sigma_Y$). Second, relatively short corrosion is projected on the shape of a parabola and long corrosion is projected on the shape of a rectangle. The failure pressure equation for the corroded pipeline is classified by parabola and rectangle as shown in Fig. 2.

Parabolic defects:

$$P_f = \frac{2(1.1\sigma_Y) \times t}{D}\left[\frac{1-(2/3)\times(d/t)}{1-(2/3)\times(d/t)/M}\right], \tag{1}$$

where $M = \sqrt{1+0.8\left(\frac{L}{D}\right)^2\left(\frac{D}{t}\right)}$, for $\sqrt{0.8\left(\frac{L}{D}\right)^2\left(\frac{D}{t}\right)} \leqslant 4$.

Rectangular defects

$$P_f = \frac{2(1.1\sigma_Y) \times t}{D}[1-(d/t)], \tag{2}$$

where $M = \infty$,

$$\text{for } \sqrt{0.8\left(\frac{L}{D}\right)^2\left(\frac{D}{t}\right)} > 4,$$

where P_f, D, d, t, M, σ_Y and L are the failure pressure, outer diameter, maximum corrosion depth, wall thickness, bulging factor, yield stress and longitudinal corrosion defect length, respectively. Due to some problems associated with the definition of flow stress a new flow stress was proposed as:

$$\sigma_f = 1.1 \times \sigma_Y + 69(\text{MPa}). \tag{3}$$

The modified ASME B31G including this new modified flow stress and bulging factor is a follows:

$$P_f = \frac{2(1.1\sigma_Y + 69) \times t}{D}\left[\frac{1-0.85\times(d/t)}{1-0.85\times(d/t)/M}\right],$$

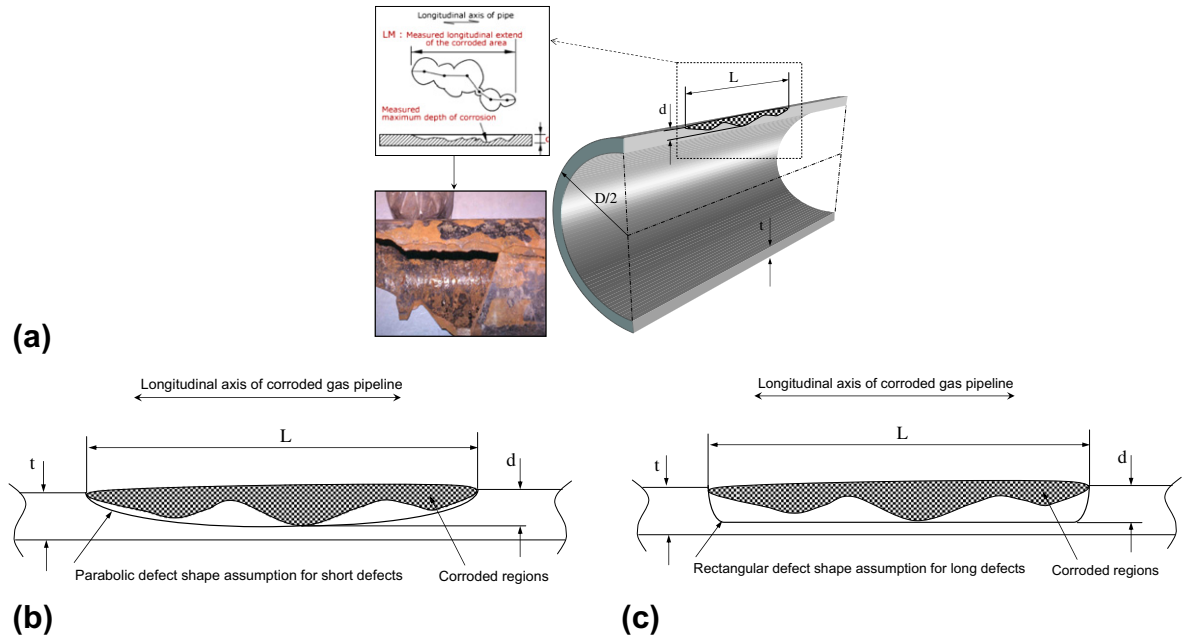

Fig. 2. (a) Typical illustration of corrosion defects (longitudinal axis). (b) Short corrosion defect simplified as a parabolic curve (ASME B31G). (c) Long corrosion defects simplified as a rectangular defect.

$$\text{where } M = \sqrt{1 + 0.6275\left(\frac{L}{D}\right)^2\left(\frac{D}{t}\right) - 0.003375\left(\frac{L}{D}\right)^4\left(\frac{D}{t}\right)^2}, \tag{4}$$

$$\text{for } \left(\frac{L}{D}\right)^2\left(\frac{D}{t}\right) \leqslant 50.$$

$$P_f = \frac{2(1.1\sigma_Y + 69) \times t}{D}\left[\frac{1 - 0.85 \times (d/t)}{1 - 0.85 \times (d/t)/M}\right],$$

$$\text{where } M = 3.3 + 0.032\left(\frac{L}{D}\right)^2\left(\frac{D}{t}\right), \tag{5}$$

$$\text{for } \left(\frac{L}{D}\right)^2\left(\frac{D}{t}\right) > 50.$$

It is necessary to recall that ASME B31G is limited to low stress concentration factors and internal pressure loading conditions. In the assessment procedure, one considers the maximum depth and longitudinal extent of the corroded area, but ignores the circumferential extent and the actual profile. If the corroded region is found to be unacceptable, B31G allows the use of more rigorous analysis or a hydrostatic pressure test in order to determine the pipe remaining strength. Alternatively, a lower maximum allowable operating pressure may be imposed.

2.2. DNV RP-F101 [2]

DNV RP-F101 is the first comprehensive and extensive code for pipeline corrosion defect assessment. It provides guidance for internal pressure and combined loading. It covers all loading types e.g., pressure only and combined loading. Furthermore, it provides codified formulations for pressure, bending and area depth. DNV RP-101 proposes two methods to find the failure pressure. The first method is based on the partial safety factor and the second is classified as allowable stress design. Both methods entail information on the pipe outside diameter (D), wall thickness (t), ultimate tensile strength (σ_u), maximum allowable operating pressure (MAOP), longitudinal extent of corrosion (L_c) and defect depth (d). The allowable stress design method considering non-interacting defects is discussed here. The exact procedures for the partial safety factor method and interacting defects can be found within the DNV code. To pursue the design procedure via DNV RP-101, it is required to determine the loading type (pressure only and combined loading) and consequently, the failure pressure can be obtained as:

$$P_f = \frac{2(\sigma_u) \times t}{(D - t)}\left[\frac{1 - (d/t)}{1 - (d/t)/Q}\right], \tag{6}$$

$$\text{where } Q = \sqrt{1 + 0.31\left(\frac{1}{\sqrt{Dt}}\right)^2},$$

where P_f, D, d, t, Q and σ_u are the failure pressure, outside diameter, corrosion depth, wall thickness, correction factor and ultimate tensile strength, respectively. According to DVN RP-101, the failure pressure should not exceed the maximum allowable stress design operating pressure (MAOP), otherwise, the corroded pipe will be repaired or replaced before returning to service.

2.3. Choi's method

Based on limit load analysis assumptions and finite element analysis of corroded pipelines, Choi et al. [3] proposed a limit load solution as a function of R/t, d/t, $L/\sqrt{Rt}$ as follows:

$$P_f = \begin{cases} 0.9 \times \frac{2(\sigma_u)\times t}{D_i}\left[C_0 + C_1\left(\frac{L}{\sqrt{Rt}}\right) + C_2\left(\frac{L}{\sqrt{Rt}}\right)^2\right], \\ \frac{L}{\sqrt{Rt}} < 6 \\ 1 \times \frac{2(\sigma_u)\times t}{D_i}\left[C_3 + C_4\left(\frac{L}{\sqrt{Rt}}\right)\right], \quad \frac{L}{\sqrt{Rt}} \geqslant 6 \end{cases}, \tag{7}$$

where P_f, σ_u, D_i, d, t and R are the failure pressure or maximum pressure, ultimate tensile strength, inside diameter, defect depth, wall thickness and average pipe radius, respectively. In general, the corrosion pits are idealized into a semi-elliptical shape rather than rectangular and semi-spherical shapes.

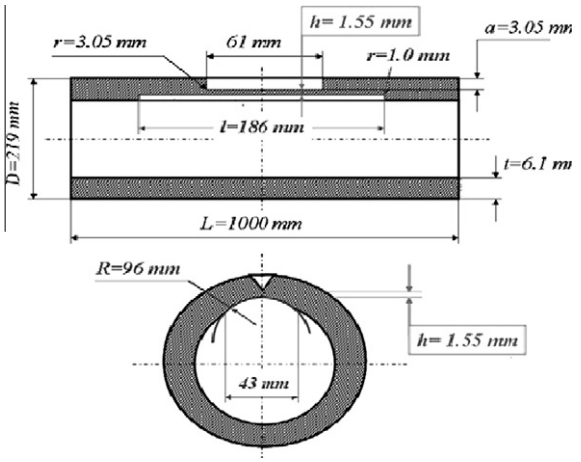

Fig. 3. Geometry of the specimens used for burst test.

$$\text{where } \left\{ \begin{array}{l} C_0 = 0.06\left(\frac{d}{t}\right)^2 - 0.1035\left(\frac{d}{t}\right) + 1, \\ C_1 = -0.6913\left(\frac{d}{t}\right)^2 + 0.4548\left(\frac{d}{t}\right) - 0.1447, \quad C_2 = 0.1163\left(\frac{d}{t}\right)^2 - 0.1053\left(\frac{d}{t}\right) + 0.0292, \\ C_3 = -0.9847\left(\frac{d}{t}\right) + 1.1101, \quad C_4 = 0.0071\left(\frac{d}{t}\right) - 0.0126 \end{array} \right\}. \tag{8}$$

2.4. Experimental verification and codes comparison

An experimental verification has been made by burst tests. Specimens are a rolled steel cylindrical pipes with an external diameter of 219.1 mm and a thickness of 6.1 mm. A quasi-semi-ellipsoidal notch represents a corrosion external defect. The major axis of the ellipsoid is parallel to the axis of the tube and the length of the notch is 30.5 mm. The depth of the notch is 3.05 mm and the width is also 3.05 mm. The radius of the notch tip is 0.15 mm, as shown in Figs. 3 and 4. A schematic view of the notched tube is given in Fig. 3.

Some tubes containing a notch with the dimensions given here were loaded with a gas up to failure (Fig. 4). Fracture occurs under a pressure of about 12 MPa. Only two results are available, but they give fracture pressures that are close together (see Fig. 5). Moreover, this type of burst test with gas is rare, as are papers on this subject. So it is very difficult to properly

Fig. 4. Experimental device for burst test under gas pressure.

Fig. 5. Specimen after fracture.

Table 1
Predicted burst pressures from codes.

	P_{uk} (MPa)	Error compared between experimental results (%)
ASME B31 G	11.3	5.8
Modified ASME B31 G	10.8	10
DNV RP-F101	6.6	45

compare our results. If we consider the gross hoop stress, it appears that computation gives a maximum value that is less than the yield strength. The hoop stress acts along the circular direction of the tube, but the stress in a perpendicular direction acts in the longitudinal direction of the tube and the strains in this direction are constrained by the great length of the tube. Consequently, a triaxiality effect is induced, and the stress to be observed is the Von Mises stress. This triaxiality effect induces an over stress to obtain the yield of the material. Here, the overstress factor is $t = \sigma_{VM}/\sigma_y = 760/528 = 1.44$. The maximum value is about 760 MPa for an internal pressure of 12 MPa.

Predicted burst pressure was determined with codes ASME B31G and DVNRP-F101 and results are reported in Table 1. According to the experimental result, it seems that the ASME B31G code is the closest. The DNVRP-F101 is the most conservative code.

3. Modified SINTAP procedure for fracture emanating from notches [4,5]

The structural integrity of corroded pipes can be made using failure assessment diagram. Classical failure assessment diagram are established for crack-like defects and are not directly applicable to corrosion defect. However a notch-adapted procedure based on notch fracture mechanics and particularly volumetric method can be used.

3.1. Volumetric method

The volumetric method [6] is a local fracture criterion, which assumed that the fracture process requires a certain volume. This volume is assumed as a cylindrical volume with effective distance as its diameter. Physical meaning of this fracture process volume is "the high stressed region" where the necessary fracture energy release rate is stored. The difficulty is to find the limit of this "high stressed region". This limit is a priori not a material constant but depends on loading mode,

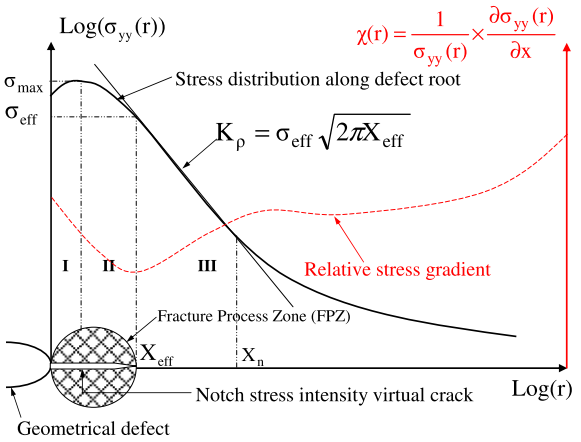

Fig. 6. Schematic elastic–plastic stress distribution along notch ligament and notch stress intensity virtual crack concept.

structure geometry and load level. The size of the fracture process reduced to the effective distance according to the above mentioned assumptions is obtained by examination of the stress distribution. The bi-logarithmic elastic–plastic stress distribution (Fig. 6) along the ligament exhibits three distinct zones which can be easily distinguished. The elastic–plastic stress primarily increases and it attains a peak value (zone I) then it gradually drops to the elastic plastic regime (zone II). Zone III represents linear behaviour in the bi-logarithmic diagram. It has been proof by examination of fracture initiation sites that the effective distance correspond to the beginning of zone III which is in fact an inflexion point on this bi logarithmic stress distribution. A graphical method based on the relative stress gradient χ associated the effective distance to the minimum of χ.

The relative stress gradient is given by:

$$\chi(r) = \frac{1}{\sigma_{yy}(r)} \frac{\partial \sigma_{yy}(r)}{\partial r}, \tag{9}$$

where $\chi(r)$ and $\sigma_{yy}(r)$ are the relative stress gradient and maximum principal stress or crack opening stress, respectively. The effective stress for fracture is then considered as the average volume of the stress distribution over the effective distance. However stresses are multiply by a weight function in order to take into account stress gradient due to geometry and loading mode. The stress distribution is given by:

$$\sigma_{eff} = \frac{1}{X_{eff}} \int_0^{X_{eff}} \sigma_{yy}(r) \times (1 - r \times \chi(r)) dr. \tag{10}$$

Therefore, the notch stress intensity factor is defined as a function of effective distance and effective stress:

$$K_\rho = \sigma_{eff} \sqrt{2\pi X_{eff}}, \tag{11}$$

where K_ρ, σ_{eff} and X_{eff} are notch stress intensity factor, effective stress and effective distance, respectively. Description of this kind of stress distribution at notch tip and the procedure with the help of the relative stress gradient is given in Fig. 6.

3.2. Notch adapted failure assessment diagram (NFAD)

An example of notch adapted failure assessment diagram is given by Matvienko [7]. The parameter k_r is defined as the ratio of the applied notch stress intensity factor K_ρ and fracture toughness K_{IC}.

$$k_r = \frac{K_\rho}{K_{IC}} = \frac{\sqrt{1 - \left(\frac{\sigma_g}{\sigma_{coh}}\right)^2}}{\sqrt{\left[1 - \left(\frac{\sigma_g}{\sigma_{coh}}\right)^2 \cdot \frac{1}{(k_t)^2}\right]}}. \tag{12}$$

Here, k_t is the elastic stress concentration factor, σ_{coh} is the cohesive stress ahead of the notch tip and σ_g the global stress.

The failure assessment curve is taken from the cohesive zone model and the criterion of average stress in the cohesive zone head of the notch tip as indicates in [7]. However the critical stress intensity factor is shown as to be a decreasing function of the elastic stress concentration factor and consequently failure assessment curve is notch radius dependant. In order to get a NFAD interpolation curve independent of the notch radius, the parameter k_r is defined as follows:

Table 2
SINTAP levels 0 and 1 description.

Level	Data needed	When to use
Default level		
Level 0	Yield or proof strength	When no other tensile data available
Standard levels		
1. Basic	Yield or proof strength: ultimate tensile Strength	For quickest result. Mismatch in properties less than 10%

$$k_r = \frac{K_{\rho,\mathrm{app}}}{K_{\rho,c}}, \tag{13}$$

$K_{\rho,\mathrm{app}}$ represents the applied notch stress intensity factor and $K_{\rho,c}$ is the critical state of the notch stress intensity factor. Another presentation of the failure criterion can be made using a two parameters relationship, $k_r = f(L_r)$, where kr is the non dimensional stress intensity factor and L_r the non dimensional load (for more detail see Ref. [4]. The fracture toughness $K_{\rho,c}$ is a function of notch radius. L_r parameter keeps the same definition. By assumption, the interpolation curve is independent of notch radius and is the same that the crack's one. Consequently, the SINTAP interpolation curves [8] were used in the NFAD.

3.3. Failure assessment curve

Two SINTAP levels are used (levels 0 and 1). Characteristics of these two levels are given in Table 2.
Level 0:

$$f(L_r) = \left[1 + \frac{L_r^2}{2}\right]^{\frac{-1}{2}} \left[0.3 + 0.7 \times e^{\left(-0.6 \times L_r^6\right)}\right], \quad \text{for } 0 \leqslant L_r \leqslant 1 \quad \text{where } L_r^{\max} = 1 + \left(\frac{150}{\sigma_Y}\right)^{2.5}. \tag{14}$$

Level 1:

$$f(L_r) = \begin{cases} \left[1 + \frac{L_r^2}{2}\right]^{\frac{-1}{2}} \left[0.3 + 0.7 \times e^{\left(-\mu \times L_r^6\right)}\right], & 0 \leqslant L_r \leqslant 1 \\ \left[1 + \frac{1}{2}\right]^{\frac{-1}{2}} \left[0.3 + 0.7 \times e^{(-\mu)}\right] \times L_r^{\frac{N-1}{2N}}, & 1 < L_r \leqslant L_r^{\max} \end{cases},$$

$$\text{where } \mu = \min\left[0.001 \times \frac{E}{\sigma_Y}, 0.6\right], \tag{15}$$

$$L_r^{\max} = \frac{1}{2}\left(\frac{\sigma_Y + \sigma_U}{\sigma_U}\right), \quad N = 0.3\left(1 - \frac{\sigma_Y}{\sigma_U}\right),$$

where, $f(L_r)$, L_r, $L_r^{\max}$, σ_Y, μ, E, σ_U and N are interpolating function, non dimensional loading or stress based parameter, maximum value of non dimensional loading or stress based parameter, yield stress, first correction factor, modulus of elasticity, ultimate stress, second correction facto, respectively.

3.4. Safety factor obtained from different defect geometry

In the failure assessment diagram, service conditions of a structure exhibiting a corrosion defect is represented by the assessment point A of coordinates $[L_r^*, k_r^*]$ in the NFAD plane (L_r, k_r). Due to the definition, L_r and k_r parameters are proportional to pressure and the loading path is linear passing through A and intercepting the failure assessment curve at point C (see Fig. 7). The safety factor is then defined as:

$$f_s = OC/OA. \tag{16}$$

Safety factor on corrosion defect have been determined for pressure service conditions of 70 bars for a gas pipe made in X52 steel (yield stress 410 MPa). Three kinds of surface defects are examined, semi-spherical, semi-elliptical and long semi-elliptical defects.

In Figs. 8a–8c, the geometrical configuration of these defects is presented. The defect depth for all models is equal to one-half of pipe wall thickness and the defect length over defect depth ratio is considered as 10 ($L/d = 10$).

The obtained notch stress intensity factors and applied internal pressure are utilized to define the required assessment points which are used in the failure assessment prediction (Table 3).

The safety factor has been determined on the Failure Assessment diagram according to the procedure described in Fig. 6.

In Table 4, different safety factors according to the SINTAP procedure are presented.

We note that all values of the safety factor are above the conventional value of 2 and consequently all the defect sizes are acceptable. The failure pressure is extracted by means of the maximum failure pressure according to the above-mentioned codes (ASME B31G, Modified ASME B31G, DNV RP-101 and Choi's method). The safety factor is determined by means of the applied pressure P_{app} over failure pressure P_f as:

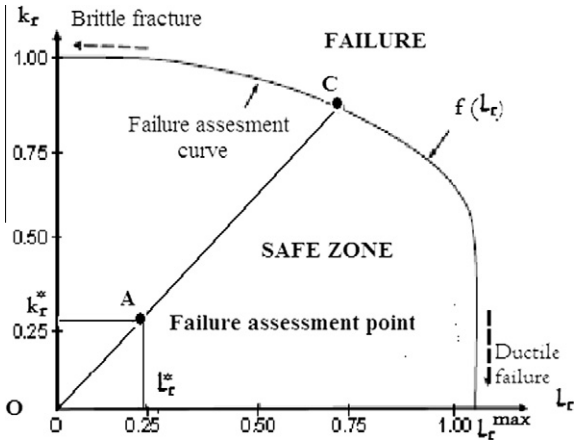

Fig. 7. Failure assessment diagram and definition of safety factor.

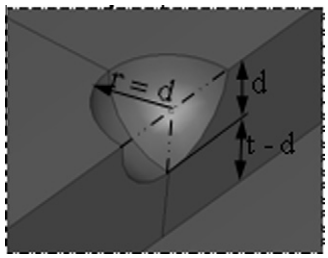

Fig. 8a. Central semi-spherical defect (t = 6.1 mm, $d = t/2$).

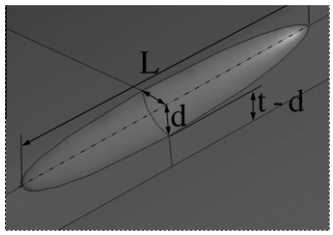

Fig. 8b. Central semi-elliptical defect (t = 6.1 mm, $d = t/2$, d/L = 0.1).

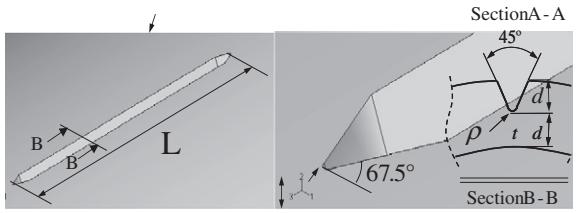

Fig. 8c. Central longitudinal semi-elliptical defect (t = 6.1 mm, $d = t/2$, d/L = 0.1, ρ = 0.15 mm).

$$F_s = \frac{P_{\text{app}}}{P_f}. \tag{17}$$

In Table 5, different safety factors according to the SINTAP procedure and limit load analysis methods are computed using implemented MATLAB code. As expected earlier, the SINTAP 0B is more conservative than SINTAP 1B. Nevertheless, ASME B31G, modified ASME B31G, DNV RP F-101 and Choi's method do not offer any structural integrity formulae for blunt notch

Table 3
Effective stress, effective distance and notch intensity factors along radial and longitudinal direction using 70 bars as applied internal pressure.

Orientation of defect	Defect type	Effective distance (mm)	Effective stress (MPa)	K_ρ (MPa $\sqrt{m}$)
Radial direction	Semi-spherical	0.42	202.7	10.4
	Semi-elliptical	0.67	343.4	22.3
	Long	0.38	539.6	26.3
Longitudinal direction	Semi-spherical	0.72	184.4	12.4
	Semi-elliptical	0.53	252.1	14.5
	Long blunt notch	0.63	311.4	19.7

Table 4
Safety factors according to the SINTAP.

Type	SINTAP 0B	SINTAP 1B
Semi-spherical	4.095	4.106
Semi-elliptical	3.407	3.750
Blunt notch	3.186	3.583

defects and DNV RP F-101 does not exhibit any variation in safety factor for the chosen semi-spherical and semi-elliptical defects. The comparison of computed safety factors emphasizes that DNV RP F-101 and Choi's method provide the upper bound and lower bound margins.

3.5. Probabilistic safety factor

On the probabilistic point of view, the failure assessment diagram can divide into zone of iso failure probabilities. The material failure curve is a particular case for which the failure probability is equal to 1 because failure is then a certainty. Any assessment point of coordinates $[L_r^* - k_r^*]$ is situated on an equi probability curve P_r^*. The following conventional failure probability are often used $P_r = 10^{-4}$ if there is no human life risk and $P_r = 10^{-6}$; if there is. These conventional iso failure probabilities divided the failure assessment diagram into three zones: the unsafe zone with $P_r = 1$; the safe zone with maintenance $P_r^* > 10^{-4}$ or 10^{-6} and the safe zone without maintenance $P_r^* < 10^{-4}$ or 10^{-6}. This type of failure assessment diagram is called probabilistic NFAD (Fig. 9).

The pipes located in a water network which consists of a pump, a reservoir and five pipe sections are submitted to a stochastic water hammer. Fracture toughness, yield stress and corrosion depth are assumed to be randomly distributed to allow determination of safety factor by Monte-Carlo and Form/Sorm methods. Within the chosen procedure, the following parameters are treated as random parameters and introduce into the notch failure assessment diagram:

- notch fracture toughness $K_{r,c}$,
- yield strength Re,
- ultimate tensile strength σ_{ult},
- defect depth a,
- maximum pressure p_{max}.

These random parameters are treated as not being correlated with one another. The exponential distribution generally governs for defect size analysis. Consequently, the probability density function has the following form:

$$F(X) = \lambda \exp(-\lambda a), \tag{18}$$

where λ is the exponential distribution parameter. The mechanical properties of the studied steel materials are presented in Table 6.

In probability theory and statistics, the variational coefficient (CV) is a normalized measure of dispersion of a probability distribution. It is defined as the ratio of the standard deviation σ to the mean μ:

$$CV = \frac{\sigma}{\mu}. \tag{19}$$

Table 5
Calculated safety factors using mentioned coded and other methods.

Type of defect	SINTAP 0B	SINTAP 1B	ASME B31G	MASME B31G	DNV RP F-101	Choi et al.
Semi-spherical	4.0	4.1	3.5	4.0	4.2	3.3
Semi-elliptical	3.4	3.7	3.4	3.9	4.2	2.8
Blunt notch	3.1	3.5	N/A	N/A	N/A	N/A

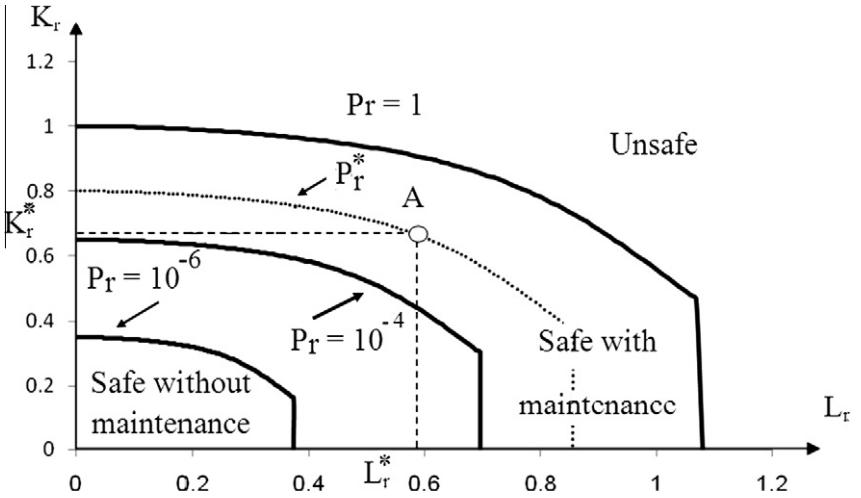

Fig. 9. Probabilistic notch failure assessment diagram (PNFAD) with definitions of material failure curve, assessment point, safe and unsafe zones and safety factor.

This is only defined for non-zero mean, and is most useful for variables that are always positive. It is also known as unitized risk or the variation coefficient. It is expressed as percentage. We have chosen the lower bound for variational coefficient, i.e. CV = 0.1. Using Monte-Carlo method, several assessment points (40–50) were generated using the characteristic parameters of the distribution. The obtained NFAD are presented in Fig. 10.

The NFAD can be presented into polar coordinates (r, θ). Two particulars value are noted in this polar diagram θ_1 and θ_2. The first polar angle θ_1 corresponds to the angle of the intercept of the failure curve at abscissa $L_r = 0.62$. This corresponds to a conventional value of gross failure stress of 62% of the yield stress. The second polar angle θ_2 corresponds to the intercept of the vertical line of $L_r^{\max}$ abscissa. These two angles determine three domains in the NFAD diagram (Fig. 11).

- If $\theta < \theta_1$ brittle fracture.
- If $\theta_1 < \theta < \theta_2$ elastoplastic fracture.
- If $\theta > \theta_2$ plastic collapse.

These three different failure zones are presented in Fig. 11. For any assessment point A we can define the safety factor according to Eq. (20).

$$f_s = OA/OB. \tag{20}$$

However, and mainly for steel and cast iron, the assessment points lay in the plastic collapse zone. Another way to define safety, is to consider that we have plastic collapse only for $\theta = 0$.

In this case the safety factor is define as:

$$f_s^* = OA^*/OB^*. \tag{21}$$

Values of θ_1 and θ_2 are respectively $\theta_1 = 55$ and $\theta_2 = 22°$. Muhammed et al. [9] have shown that the general trend that emerges is that on average the margin of safety on the FAD is minimum in the middle (elastic–plastic) region, slightly higher in the 'plastic collapse region and maximum in the 'fracture' region. However, this overall trend is complicated by varying degree of scatter in the different regions. For this reason, we have examined the evolution of the safety factor with the θ angle. It has been shown that the θ angle is in range [0–7°] for steel, [0–15°] for cast iron and [0–4°] for polyethylene. All

Table 6
Mechanical properties of pipe steel and used distribution.

Mechanical properties	Yield strength (Re)	Ultimate strength	Circumferential stress	Fracture toughness	Defect
Mean	410 MPa	528 MPa	41.8 MPa	116 MPa $\sqrt{m}$	2 mm
CV	0.1	0.1	0.4	0.1	–
Stresses/SIF	41 MPa	52.8 MPa	18.44 MPa	11,6 MPa $\sqrt{m}$	–
Distribution	Normal	Normal	Normal	Weibull	Exponential

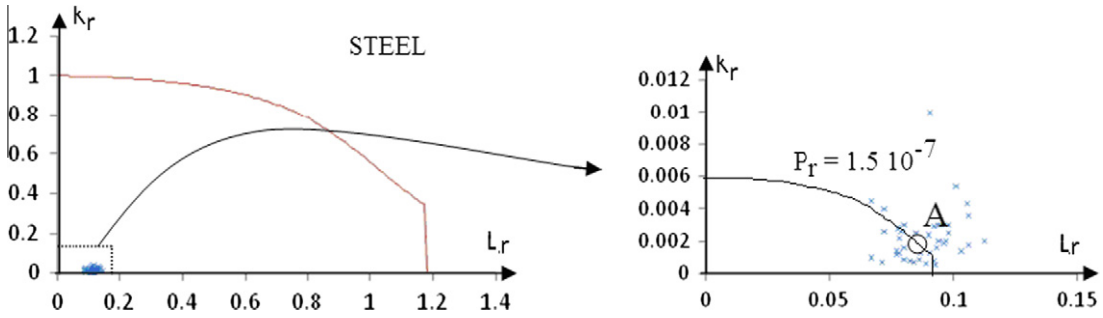

Fig. 10. Example of probabilistic notch failure assessment diagram for steel.

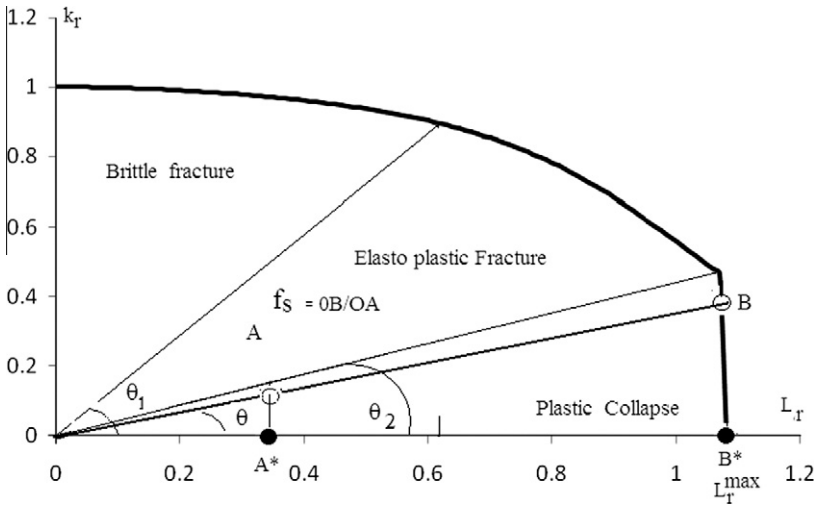

Fig. 11. Definition of zones of brittle fracture, elasto plastic failure and plastic collapse in NFAD and definition of theta angle.

data are in a narrow scatter band of range $[\mu - 3\sigma;\ \mu + 3\sigma]$ and in the region of plastic collapse. For this reason the safety factor f_s^* computed from the ultimate pressure done by code ASME B31G is also reported (Fig. 12). Mean values and standard deviation for the safety factor of the three material are reported in Table 7.

The safety factor computed for fully plastic collapse is less than the mean value of f_s.

The safety factor distribution is represented with a Weibull distribution. Kolmogorov–Smirnov test results indicates (see Table 7) that the Weibull distribution is significant at 57%.

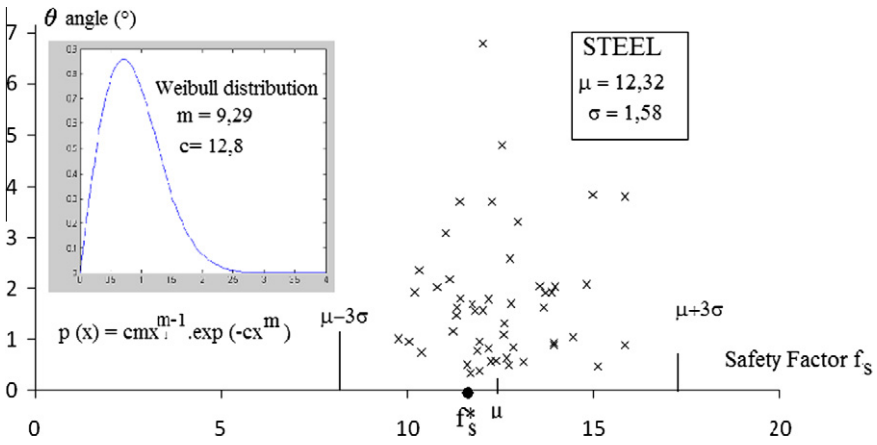

Fig. 12. Distribution of the safety factor with q angle for pipe steel.

Table 7
Mean values and standard deviation for the safety factor of the material.

Material	Steel
Mean μ	12.32
f_s^*	11.63
Standard deviation σ	1.26
Variational coefficient CV	0.12

4. Conclusion

The structural integrity of corroded pipelines subjected to internal pressure is studied in this paper. The semi-spherical, semi-elliptical and blunt notch defects are examined under this loading and safety factors are evaluated by means of the SINTAP procedure which is modified using a notch-based failure assessment diagram or so-called "NFAD". The ASME B31G, modified ASME B31G, DNV RP F-101 and Choi's method have been also utilized.

The values of deterministic safety factor are codified in codes such as EUROCODE 3 [10]. However, the actual trend is to adopt partial safety factor according to the degree of uncertainties of the material properties in order to avoid over conservatism. The design material properties are then defined as some percentile of the material resistance distribution (the mean values is generally used for metals and alloy but for wood the admissible stress is defined as the 5th percentile of the distribution). The use of probabilistic notch failure assessment diagram allows getting global safety factor without introducing a series of partial safety factors on material properties, defect size and applied loading. In addition, the probabilistic safety factor is associated to a failure probability. Then, with a conventional allowed failure probability, it is possible to have a maintenance policy and to compute the economic cost of the risk of structure failure. Under stochastic service pressure, the safety factor is distributed randomly according to Weibull distribution. It has been seen that the Weibull modulus of the distribution is about 10 and the confidence interval of the safety factor has a satisfactory value.

References

[1] American National Standard Institute (ANSI)/American Society of Mechanical Engineers (ASME). Manual for determining strength of corroded pipelines, ASME B31G; 1984.
[2] DNV RP-F101 (2) DNV-RP-F101: Corroded pipelines. Det Norske Veritas; 1999.
[3] Choi JB, Goo BK, Kim JC, Kim YJ, Kim WS. Development of limit load solutions for corroded gas pipelines. Int J Pres Ves Piping 2003;80(2):121–8.
[4] Hadj Meliani M, Azari Z, Pluvinage G, Capelle J. Gouge assessment for pipes and associated transferability problem. Eng Fail Anal 2010;17:1117–26.
[5] Moustabchir H, Azari Z, Hariri S, Dmytrakh I. Experimental and numerical study of stress–strain state of pressurised cylindrical shells with external defects. Eng Fail Anal 2010;17:506–14.
[6] Pluvinage G. Fracture and fatigue emanating from stress concentrators. Kluwer; 2003.
[7] Matvienko YG. Local fracture criterion to describe failure assessment diagrams for a body with crack/notch. Int J Fract 2003;124:107–12.
[8] Structural integrity assessment procedure (SINTAP). Final report EU project BE95-1462 Brite Euram Programme Brussels; 1999.
[9] Muhammed A, Pisarski HG, Sanderson RM. Calibration of probability of failure stimates made from probabilistic fracture mechanics analysis. Offshore technology report, 2000/021. TWI Ltd.; 2000.
[10] Eurocode 3. Design of steel structures. General rules and rules for buildings division 1. Class 1; 2005.